Adsorption (2024) 30:673–684
https://doi.org/10.1007/s10450-024-00459-6

Tailoring hydrophobicity vs. water capacity of adsorbents for adsorption applications: role of composites

Cigdem Atalay-Oral[1] · **Melkon Tatlier**[1]

Received: 4 December 2023 / Revised: 19 March 2024 / Accepted: 20 March 2024 / Published online: 7 April 2024

Abstract
Water adsorption capacities of various adsorbents reported in the literature were investigated to define a hydrophobicity index that was plotted vs. water capacity. In this plot, logarithmic curves were proposed to be used as indicators of performance limits of adsorbents, especially for adsorption heat pumps. In spite of their useful adsorption properties, zeolites generally exhibited quite low hydrophobicity, remaining well below the logarithmic curve. In this study, the use of composites of zeolite NaY was examined both theoretically and experimentally for improvements in the water capacity and hydrophobicity. Salt impregnation and hydrothermal synthesis experiments were performed to prepare composites of zeolite NaY with LiCl/$MgCl_2$ salts and activated carbon, respectively. Water capacity and hydrophobicity of zeolite NaY composites were generally superior to those of pure zeolite. Zeolite composites may be advantageous for enhancing adsorption capacity and hydrophobicity of zeolites while eliminating low stability and slow adsorption kinetics of other adsorbents. Interface between two different phases might indicate another opportunity to provide improved adsorption properties for zeolite composites.

Keywords Composite · Adsorption · Hydrophobicity · Zeolite · Salts · Activated carbon

1 Introduction

Seeking an adsorbent with high water capacity and low regeneration temperature (requiring some hydrophobicity) is crucial for obtaining high performance from systems involving water sorption, such as adsorption heat pumps/cooling systems and desiccant dehumidifiers. The hydrothermal stability of the adsorbent as well as the shape of the adsorption isotherm, determining the amount of adsorption in a certain P/P_0 range, also affect the performances of sorption systems.

Water sorption systems may use a variety of adsorbent materials, such as silica gel, activated carbon, salts, mesoporous silicates, clays, zeolites and metal organic frameworks (MOF). Silica gel has the advantages of being a low cost material with relatively low regeneration temperature, while the linear shape of its adsorption isotherm for water may bring some limitations to its use. Activated carbon has large pore volume and high surface area with an S-shaped type V water adsorption isotherm. Mesoporous silicates may have large surface areas and type V adsorption isotherms while natural mineral clays may be commercially available with relatively low cost. The water adsorption capacities of hygroscopic salts, such as haloids, nitrates and sulphates are higher than many of the adsorbents available. On the other hand, hygroscopic salts are not stable, especially under high humidity ratios. Wetting of the salt material leads to reduction in sorption performance and even loss of the adsorbent. Metal–organic frameworks (MOFs) are composed of different metal ions and organic ligands. They may have high surface areas and large pore volumes, often resulting in high water adsorption capacities. However, since adsorption of several MOFs occur at relatively high P/Po values, useful water exchange may be low for systems, such as adsorption heat pumps. Additionally, they may exhibit degradation after numerous adsorption–desorption cycles. The adsorption kinetics of these materials may also be relatively slow and further research is required for improving them. Zeolites are crystalline aluminosilicates of alkali or alkali earth elements. They have type I water adsorption isotherms,

✉ Melkon Tatlier
tatlierm@itu.edu.tr

[1] Department of Chemical Engineering, Istanbul Technical University, Maslak, Istanbul 34469, Turkey

typical of microporous materials, regarded as very suitable for adsorption heat pumps and similar systems. They have large surface areas, fast adsorption kinetics and are hydrothermally stable. There are different types of zeolites, ranging from very hydrophilic to hydrophobic. The adsorption amount is generally higher for hydrophilic zeolites, such as A and X, represented by lower Si/Al ratios. However, hydrophilic zeolites can be regenerated at relatively higher temperatures generally above 150 °C, due to the strong bond of water molecules with Al in the zeolites. Aluminophosphate (AlPO), silicoaluminophosphate (SAPO) and ferroaluminophosphate (FAPO) zeolites also exist. These materials possess S-shaped type V water adsorption isotherms, different from aluminosilicate zeolites. Accordingly, they have relatively low regeneration temperatures. However, these materials are generally synthesized by using organic templates, which are not economical and may also present environmental problems.

Preparing composite materials may be useful to obtain adsorbents with enhanced performances. Improvement with respect to distinct adsorbents constituting the composite may be assured in case some limiting properties of the adsorbents are eliminated. One example is to form composites by applying salt impregnation to the pores of porous materials, which are used as hosts. The composite adsorbents obtained can make use of the superior sorption characteristics of hygroscopic salts and stability of other adsorbents [1]. In this manner, deliquescence may be eliminated to a great extent since the dissolved salt may remain in the pores of its host. Preparing composites by salt impregnation has been investigated for a variety of adsorbents. Silica gels [2], mesoporous silicates [3], activated carbons [4], MOFs [5] and clays [6] profited from salt impregnation, mainly by increases in water capacity and partly by decreases in regeneration temperature. Salt impregnation provided enhancements in the water capacities of a few zeolites as well. These included NaX (aluminosilicate) [7, 8] and SAPO-34 (silicoaluminophosphate) [9] zeolites. Optimum amount of salt loading was determined to exist [8]. The stability varied with different materials and conditions used. After numerous cycles, some reduction was observed in the water capacities of some of the composites [8], while in other cases, the modified zeolites had good thermal stabilities and no obvious capacity loss [7]. Some observations of composites exhibiting decreased sorption rate, when compared to the pure zeolite, were also made [7].

Some studies have also been performed to prepare composites of activated carbon and zeolite. In some of these, activated carbon was added to the zeolite synthesis mixture where crystallization took place [10–12]. However, raw materials, such as coal gangue and metakaolin or organic templates were generally used to obtain the zeolite in these cases. Other studies involved the preparation of composites by mixing zeolite and activated carbon powders, followed by various activation procedures [13, 14]. Zeolites and activated carbons are useful adsorbents for CO_2 adsorption, due to their high adsorption capacity and selective CO_2 adsorption. Zeolites, as microporous aluminosilicates with crystalline structures, are cost effective and have high hydrothermal stability while activated carbons have pore size distribution, low cost, low heat of adsorption and are rather hydrophobic. Composites of zeolite and activated carbon with enhanced porosity and adsorption capacities for CO_2 and CH_4 could be prepared [13]. Zeolite-activated carbon composites were also observed to have significant adsorption capacities for eliminating cationic dyes [14] and heavy metal ions [10] from industrial wastewater. On the other hand, the use of such composites for water adsorption was not investigated.

In this study, firstly, the water adsorption capacities of various adsorbents reported in the literature were investigated and a hydrophobicity index was defined, especially considering adsorption heat pump applications. A logarithmic curve was proposed in order to describe the competency of water adsorption performances of various adsorbents, by taking into consideration the relation between water adsorption capacity and hydrophobicity. The situation for zeolites was highlighted and NaY zeolite was investigated both theoretically and experimentally for possible improvements that might occur when its composites were formed. This silicoaluminate zeolite was selected for contributing new materials and data to the literature, as well as due to its relatively high water capacity. Salt impregnation was carried out to form composites of zeolite NaY with LiCl and $MgCl_2$ salts. Hydrothermal synthesis and a clear homogeneous reaction mixture (prepared without using organic templates but only basic reactants) were utilized to obtain zeolite Y-activated carbon composites. The materials obtained were characterized by X-ray diffraction (XRD), field emission gun scanning electron microscopy (FEGSEM), energy dispersive X-ray spectroscopy (EDX) and thermogravimetry (TG). The water capacities of the composites at relatively low and high temperatures as well as their hydrophobicity, as obtained by thermogravimtery, were compared to those of the pure adsorbents.

2 Determination of hydrophobicity vs. water capacity of adsorbents

Adsorption data presented in the literature were investigated for silica gels, activated carbons, zeolites, hygroscopic salts, metal organic frameworks (MOFs), clays, coals, graphene oxides, mesoporous silicates and xerogels [15–61]. Water adsorption capacities of the adsorbents at different P/P_0

values were noted. In the literature, water adsorption, hydrocarbon/water adsorption and thermogravimetry have been reported as methods for the determination of hydrophobicity of adsorbents [62]. In this study, two hydrophobicity indexes were calculated. The first one, HI_1, was obtained by subtracting the ratio of the water adsorption capacities at $P/P_0 = 0.1$ and $P/P_0 = 0.9$ from 1 (Eq. 1). The second index, HI_2, was related to thermogravimetry measurements and was equal to the ratio of water capacities measured at 100 °C and at 350 °C (Eq. 2).

$$HI_1 = 1 - C_{0.1}/C_{0.9} \quad (1)$$

$$HI_2 = C_{100}/C_{350} \quad (2)$$

The aim for using HI_1 was to assess the hydrophobicity of adsorbents according to a given P/P_0 value (e.g., 0.1) while an ultimate decision about hydrophobicity was not intended to be made. The P/P_0 value of 0.9 corresponded to the total adsorption capacity. Such a specific investigation may become more meaningful when we consider the existence of different applications of adsorption. For example, a P/P_0 value of 0.1 is critical for the adsorption heat pump application, thus, the hydrophobicity values of the adsorbents determined in this study may be regarded as representatives for this application. Some other P/P_0 values may provide different hydrophobicities more suitable to represent other applications. The hydrophobicity index HI_2 represented the ratio of the amount of water desorbed from the adsorbent at 100 °C to the total water capacity. For this index, when the temperature of 100 °C, which is the critical parameter corresponding to the available heat for the regeneration of the adsorbent, is changed to another value, somewhat different results may be obtained for the hydrophobicity. In this study, the temperature of 100 °C was selected by taking into consideration adsorption heat pump applications, too.

HI_1 index was plotted vs. water adsorption capacity near saturation, $C_{0.9}$. Additionally, HI_1 index was recalculated in such a manner that would allow the adsorption of 0.15 g/g adsorbent at $P/P_0 = 0.1$, for each adsorbent data. This capacity value may be further varied according to the target application and has been given as a reasonable example, especially considering adsorption heat pumps, in this study. The logarithmic curve passing through the points obtained by recalculation may be used as an indicator of the competency of water adsorption performances of various adsorbents.

Zeolite NaY has one of the highest water adsorption capacities among aluminosilicate zeolites while it is somewhat more hydrophobic than the ones with similar capacities. Some aluminophosphate zeolites exhibit higher hydrophobicity with similar water capacity, but they are generally synthesized by using organic templates, which may present economical and environmental problems, as mentioned before. Zeolite NaY may be synthesized without using organic templates. In this study, this zeolite was taken as a basis for the studies performed to investigate possible changes that may occur in the water capacity and hydrophobicity of zeolites when their various composites are formed. For this aim, firstly, the adsorption performances of the composites of NaY zeolite prepared by using MCM-41 (mesoporous silicate), montmorillonite (clay), activated carbon, MIL-101 (MOF), silica gel and LiCl (salt) were calculated by using literature adsorption data. The adsorption capacity of the composite was calculated as the average of the two different materials constituting the composite while the HI_1 index of the composite was determined by using Eq. (1), where the capacities at $P/P_0 = 0.1$ and $P/P_0 = 0.9$ were both average values of the two different materials constituting the composite. A merely theoretical investigation was made which did not take into account any synergistic effect, but only simple physical mixing of the distinct adsorbents.

3 Experimental

3.1 Preparation of zeolite-salt composites

Composites of zeolite NaY were formed by using hygroscopic salts and activated carbon in this study. For the first case, powder zeolite NaY was impregnated with $MgCl_2$ or LiCl in order to investigate the changes in the adsorption properties of this zeolite when its composites were prepared. Commercial zeolite NaY1 powder (Aldrich) and a procedure described in the literature were used for the salt impregnation performed [7]. Accordingly, the zeolite was immersed in a $MgCl_2$ (Merck) or LiCl (Merck) solution (5 wt%), where it was kept for 24 h at room temperature. The zeolite/salt mass ratio was equal to 20/3. Then, the mixture was evaporated at 80 °C, so that the water could be removed and the residual $MgCl_2$ or LiCl could be adsorbed on the zeolite surface. Under these conditions, it was stated that a large proportion of the salt may penetrate into the micropore while others may occupy the mesopores or macropores outside the zeolite crystals [7]. On the other hand, the use of salts led to only minor amount of ion exchange in the zeolite [7]. The composites were named as NaY1-LiCl and NaY1-$MgCl_2$.

3.2 Preparation of zeolite-activated carbon composites

The second task was the preparation of zeolite-activated carbon composites. For this aim, activated carbon powder

(Aldrich) was added to a zeolite synthesis mixture with a molar composition of 42.5 Na_2O: 1 Al_2O_3: 17 SiO_2: 850 H_2O [63]. This reaction mixture composition was originally demonstrated to lead to the formation of mainly zeolite NaY with smaller amount of zeolite NaA [63]. The reaction mixture was prepared by using granular sodium aluminate (Riedel-de Haen, > 99%), sodium silicate (Merck, extra pure), anhydrous sodium hydroxide pellets (Merck, > 97%) and deionized water. The clear synthesis solution formed was kept on a magnetic stirrer for about 10 min. After the inclusion of the activated carbon powder, hydrothermal synthesis was performed in an oven kept at 80 °C for 24 h. After synthesis, the solution was filtered and the grayish powder obtained was dried overnight in an oven at 80 °C. Two different activated carbon amounts of 0.15 g and 0.30 g were used in the experiments while the synthesis mixture was equal to about 95 g in both cases. The resulting powder mass was equal to 1.35 g and 1.60 g for the use of lower and higher amounts of activated carbon. The composites were named as NaY2-AC1 and NaY2-AC2 for the former and latter cases, respectively.

3.3 Characterization techniques

The composites prepared were characterized by X-ray diffraction (XRD), energy dispersive X-ray (EDX) spectroscopy, field emission gun scanning electron microscopy (FEGSEM) and thermogravimetry (TG). XRD (Bruker-D8-Advance) was used for crystallinity and phase identification. CuKα radiation and a step size of 0.02° with 1.0 s per step were used. Field emission gun scanning electron microscopy (JEOL JSM-7000 F) was used to investigate the morphology of the pure and composite samples. The Oxford X-Max 20 energy dispersive X-ray (EDX) spectroscopy detector attached to the FEGSEM was used to perform elemental mapping analysis of the samples. The Na reduction degree as well as salt or carbon content were determined from the atom content of the zeolite composites. Thermogravimetric analysis (Shimadzu TA-503) was performed to determine the amount of water desorbed from the adsorbents between ambient temperature and 350 °C under nitrogen flow. A heating rate of 20 °C/min was used. Prior to the TG measurements, the samples were kept in a desiccator containing saturated NH_4Cl solution and their hydrated masses were reported. The average error in TG measurements was equal to about 1%, representing a range of error of about ±0.002 g/g adsorbent for the water capacities reported in this study. Two consecutive TG experiments were performed for each sample to obtain information about the stabilities of the composites.

4 Results and discussion

4.1 Hydrophobicity vs. water capacity of adsorbents

Figure 1 shows the variation of hydrophobicity index, HI_1, with respect to water adsorption capacity for various adsorbents. Adsorption data were obtained from the literature, as mentioned before. It may be seen from the figure that most of the adsorbents had quite high hydrophobicity while the relatively high water adsorption capacities generally pertained to salts and MOFs. On the other hand, the lowest hydrophobicity indexes mostly were those of aluminosilicate zeolites. Some MOFs also had similarly low values, though most of them were notably hydrophobic. When the water adsorption capacities were taken into consideration, zeolites remained

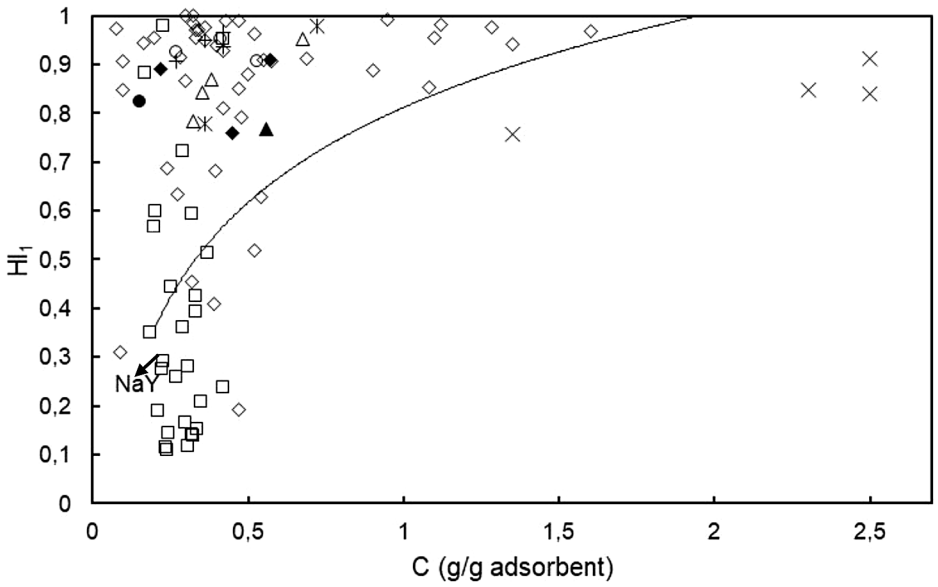

Fig. 1 Variation of hydrophobicity index, HI_1, with respect to water adsorption capacity for (▢) zeolite, (◊) MOF, (Δ) silica gel, (+) activated carbon, (x) salt, (o) clay, (▲) graphene oxide, (Ж) mesoporous silicate, (●) xerogel and (♦) coal adsorbents

within the average range of most adsorbents, excluding MOFs and salts. A logarithmic curve represented the relation between water adsorption capacity and hydrophobicity index, when a water capacity of 0.15 g/g adsorbent was assumed to exist at $P/P_0 = 0.1$, for each adsorbent. A water adsorption capacity of 0.15 g/g adsorbent may be considered suitable to provide the required useful effect for some applications, such as adsorption heat pumps and cooling systems. It may be observed from Fig. 1 that most of the adsorbents remaining below this logarithmic curve were zeolites. This indicates that zeolites may provide the targeted water capacity even at higher hydrophobicity values, pointing to the usefulness of improving their water adsorption properties further. It should be reminded that higher hydrophobicity means lower regeneration temperatures for the adsorbents. Salts also remained below the logarithmic curve. Since both their water adsorption capacity and hydrophobicity were rather high, a similar improvement for salts may be quite limited. Similar curves may be obtained for water capacities other than the 0.15 g/g adsorbent at $P/P_0 = 0.1$ used in this study to exhibit the competency of adsorption performances of various adsorbents in different applications.

Zeolites have unique properties which promote their use in many different applications, mainly related to ion-exchange, catalysis, separation and adsorption. Some significant aluminosilicate zeolites, such as A and X type are highly hydrophilic. Although being hydrophilic favors the water adsorption capacities of zeolites, it also renders them to have relatively high regeneration temperatures. Thus, introducing some hydrophobicity to these materials without leading to significant reduction in their water capacities may be beneficial. X and Y type zeolites have the same framework structure (FAU) and are called faujasites. Zeolite Y is somewhat more hydrophobic than the X type, but still has a relatively high regeneration temperature. It is synthesized in Na form after which it may be transformed into other forms by ion exchange. In this study, the adsorption performances of some composites of zeolite NaY were determined by calculation. The results are shown in Fig. 2, which depicts the variation of the hydrophobicity index, HI_1, with respect to water adsorption capacity for NaY zeolite, MIL-101 (MOF), MCM-41 (mesoporous silicate), LiCl (salt), montmorillonite (clay), silica gel, and activated carbon as well as their composites. It may be observed that the hydrophobicity indexes of the composites were much higher than that of zeolite NaY. The water adsorption capacities of the composites, especially those using MCM-41, MIL-101 and LiCl were also higher than that of the pure zeolite. The zeolite NaY composites were located very near to the logarithmic curve proposed in this study, with the exception of NaY-LiCl composite. Although situated below the curve, NaY-LiCl exhibited the highest water capacity by far among the composites. The highest hydrophobicity indexes pertained to NaY-MIL-101 and NaY-MCM-41 composites, though the differences were not big.

4.2 Zeolite NaY-salt composites

In this study, composites of NaY zeolite and LiCl or $MgCl_2$ were prepared by salt impregnation. Figure 3a, b and c show the FEGSEM pictures of zeolite NaY1, NaY1-LiCl composite and NaY1-$MgCl_2$ composite, respectively. The characteristic octahedral morphology of Y zeolite (faujasite) may be observed in all pictures. The composites looked as crystalline as the original zeolite. The pore size of zeolite NaY is equal to 7.4 Å, so the salts may enter the micropores

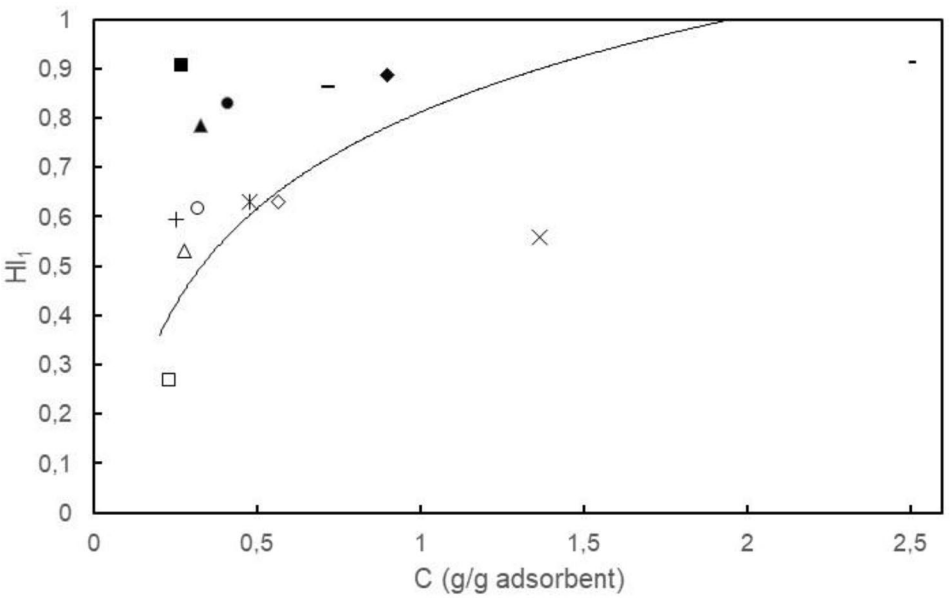

Fig. 2 Variation of the hydrophobicity index, HI_1, with respect to water adsorption capacity for (▢) NaY zeolite, (♦) MIL-101, (●) montmorillonite, (▲) silica gel, (■) activated carbon, (—) MCM-41, (-) LiCl, (◊) NaY-MIL-101 composite, (o) NaY-montmorillonite composite (+) NaY-activated carbon composite, (Δ) NaY-silica gel composite, (x) NaY-LiCl composite and (Ж) NaY-MCM-41 composite

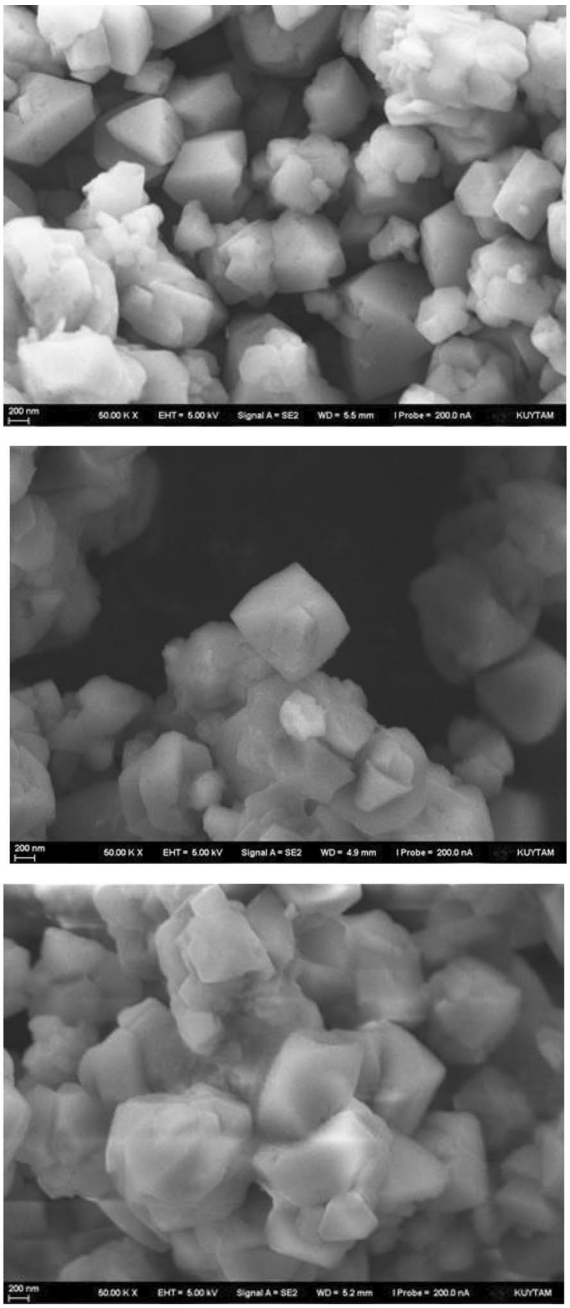

Fig. 3 FEGSEM pictures of (a) zeolite NaY1, (b) NaY1-LiCl composite and (c) NaY1-$MgCl_2$ composite

Table 1 Amount of salt (LiCl/$MgCl_2$) by wt. and degree of reduction of Na in the composite samples

Sample	Salt content (wt%)	Degree of Na reduction
NaY1-LiCl	4.5	0.36
NaY1-$MgCl_2$	6.0	0.32

of the zeolite. They may be adsorbed on the inner or outer surfaces of the zeolite. EDX results are reported in Table 1, where the amounts of LiCl and $MgCl_2$ in the composites and reduction degree of Na, when compared to the original zeolite, may be seen. The results indicate that about 6 wt% $MgCl_2$ and 4.5 wt% LiCl were incorporated into the zeolite. Additionally, decreases were observed in the Na/Al ratios, when compared to the pure zeolite, in both cases. The reduction of Na in the composites could be related to some amount of Li and Mg ion exchange, releasing Na from the samples and also to some of the Al atoms in the zeolite framework becoming extraframework atoms. In zeolites, Na atoms reside near Al atoms in the framework structure. The Si/Al ratio of NaY zeolite was determined to be equal to about 3.2. This ratio increased very slightly for the composites and attained 3.3.

TG curves of zeolite NaY1 as well as NaY1-LiCl and NaY1-$MgCl_2$ composites are given in Fig. 4. It may be observed that the highest and lowest water capacities were obtained for the NaY1-LiCl composite and pure NaY1 zeolite, respectively. The situation did not change at both relatively high and low temperatures. Desorption kinetics did not seem to be slow for the zeolite-salt composites, but adsorption kinetics should also be checked. The amounts of water desorbed from the samples were noted at 100 °C and 350 °C in the TG measurements. The water capacities are given in Table 2. It may be observed from the table that after salt impregnation, the highest water capacity at both 100 °C and 350 °C pertained to the NaY1-LiCl composite. The water capacity of this composite was higher than that of zeolite NaY1 by about 10% and 53% at the relatively high and low temperatures, respectively. Improvement was also observed for the NaY1-$MgCl_2$ composite, by about 6% and 36% at the relatively high and low temperatures, respectively. The significant amount of increase at the lower temperature of 100 °C indicated enhanced hydrophobicity for the zeolite-salt composites, especially for NaY1-LiCl. The hydrophobicity index, HI_2, increased by about 39% and 29% for the composites prepared by using LiCl and $MgCl_2$, respectively, when compared to that of pure NaY1 zeolite. The hydrophobicity index of zeolite NaY1 determined by thermogravimetry in this study ($HI_2 = 0.296$) was quite similar to the hydrophobicity index ($HI_1 = 0.290$) obtained from adsorption data [15]. The water capacity of about 0.24 g/g zeolite determined at 350 °C in TG measurements was also similar to literature adsorption capacity values. It is not possible to say that the two hydrophobicity indexes will always be similar since they may sometimes pertain to different pressure/temperature ranges, as determined by the related parameter values used. Since the adsorption heat pump application was primarily taken into consideration in this study, the parameter values were selected accordingly

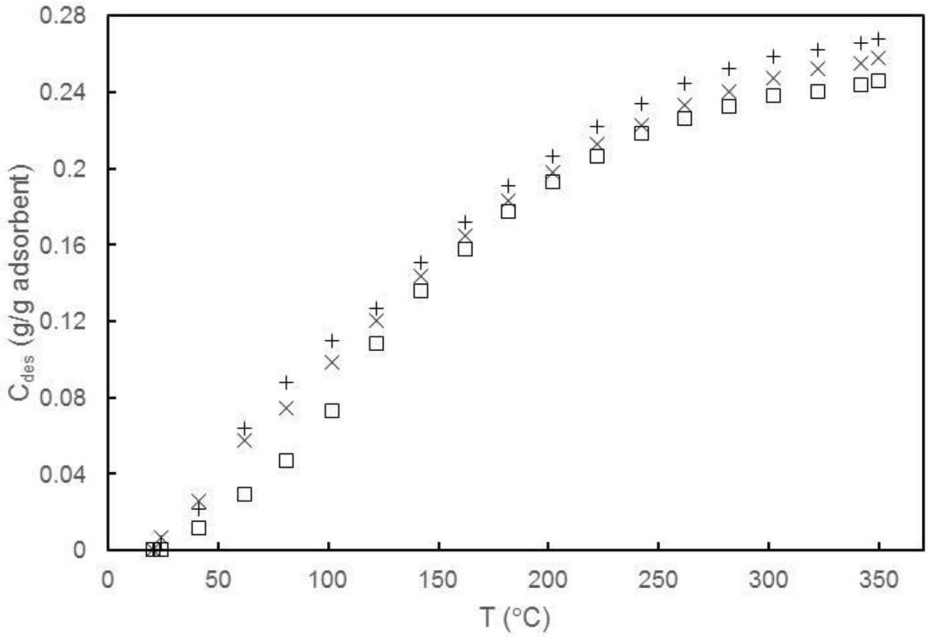

Fig. 4 TG curves of (▢) zeolite NaY1, (+) NaY1-LiCl composite and (x) NaY1-$MgCl_2$ composite

Table 2 Water capacities at 100 °C and 350 °C and HI_2 hydrophobicity index of NaY zeolite and its composites, as obtained by thermogravimetry

Sample	C_{100} (g/g adsorbent)	C_{350} (g/g adsorbent)	HI_2
NaY1	0.0720	0.243	0.296
NaY1-LiCl	0.110	0.268	0.410
NaY1-$MgCl_2$	0.0983	0.258	0.381
AC	0.120	0.145	0.827
NaY2	0.0534	0.203	0.263
NaY2-AC1	0.0608	0.223	0.274
NaY2-AC2	0.0556	0.213	0.261

and thus the two hydrophobicity indexes may be expected to have some proximity. When the logarithmic curve in Fig. 1 is taken into consideration, zeolite NaY remained well below the curve with its HI_1 and water capacity values of about 0.29 and 0.23 g/g zeolite, respectively, according to adsorption data. Since HI_1 and HI_2 were quite similar, the NaY1-LiCl composite may be deduced to have approached significantly to the limiting logarithmic curve in Fig. 1, with its hydrophobicity and water capacity values attaining about 0.41 and 0.27 g/g adsorbent, respectively. Two consecutive TG measurements were performed for each zeolite-salt composite. No significant change was observed in the water capacities, indicating the stability of the zeolite crystal structure after salt impregnation and two TG heating treatments at 350 °C.

Calculations were also made by using the total water capacities of the original NaY1 zeolite and LiCl, $MgCl_2$ salts and their weight percentages to estimate water capacities for the composites at the higher temperature of 350 °C. Water capacities of 1.35 g/g LiCl [8], 1.24 g/g $MgCl_2$ [62] and 0.24 g/g NaY1 zeolite were used in the calculations for the pure adsorbents. When NaY1 zeolite and LiCl salt were taken into account, the increase in the water capacity of the composite (at the higher temperature), when compared to zeolite NaY1, was calculated to be equal to about 20%. This was higher than the 10% increase obtained for the composite prepared by salt impregnation experimentally. The situation was similar for $MgCl_2$ and the enhancement in the water capacity of the mixture/composite at the higher temperature, when compared to zeolite NaY1, was calculated to be equal to about 24%, which was higher than the 6% increase obtained for the composite prepared by salt impregnation experimentally. These results indicate that some interactions existed between the salt and impregnated zeolite and the positive impact of salt impregnation on the water capacity of the zeolite might be limited by certain factors, such as partial pore blocking of the zeolite by the salt.

In a previous study, Li and Mg ion exchanges were applied to the same NaY zeolite. The water capacities at 350 °C, as determined by thermogravimetry, were not much different from those of the composites obtained by Li and Mg salt impregnation [63]. However, the water capacity at 100 °C and the HI_2 index were notably lower for the samples obtained by ion-exchange. Water capacities of about 0.078 g/g zeolite and 0.056 g/g zeolite were determined at 100 °C for Y zeolite after Li and Mg ion exchanges, respectively [63]. On the other hand, the NaY1-LiCl and NaY1-$MgCl_2$ composites prepared in this study by salt impregnation had water capacities at 100 °C of about 0.11 g/g adsorbent and 0.10 g/g adsorbent, respectively. The hydrophobicity index, HI_2, was around 0.4 when salt

impregnation was carried out, while it was equal to about 0.22 and 0.31 after Mg and Li ion exchanges, respectively.

4.3 Zeolite NaY-activated carbon composites

Figure 5 shows the XRD patterns of the zeolite NaY-activated carbon composites as well as the original zeolite, all obtained by synthesis experiments. It may be observed from the figure that all the samples were quite crystalline and there was little difference between the XRD patterns of the original zeolite (Fig. 5a) and zeolite composites prepared by using lower (Fig. 5b) and higher (Fig. 5c) amounts of activated carbon. The zeolite synthesis mixture used in this study originally allowed the formation of zeolite NaY along with a minor phase of zeolite NaA. The XRD peaks in Fig. 5 were indexed in accordance with the peaks reported for simulated XRD patterns of zeolites [64] and the peaks with highest intensity were marked (as A for zeolite A and as Y for zeolite Y). It is obvious that the XRD peaks of the original zeolite were also present in the XRD patterns of the zeolite-activated carbon composites. The only difference was the presence of hydroxysodalite (HS) zeolite peaks with relatively low intensity, for the NaY2-AC2 composite obtained by using the higher amount of activated carbon.

FEGSEM pictures of the NaY2-activated carbon composites and original activated carbon are given in Fig. 6. The FEGSEM picture of the original activated carbon may be seen from Fig. 6a, mostly revealing the amorphous nature of this material. In the NaY2-AC1 composite sample (Fig. 6b), octahedral zeolite Y (faujasite) crystals still prevailed while some amorphous activated carbon also existed, distributed among the zeolite crystals, forming clusters of various lengths. The same was also generally true for the NaY2-AC2 composite sample (Fig. 6c). The visible amount of activated carbon did not seem to increase for this sample, the preparation of which involved higher amount of activated carbon.

TG curves of zeolite NaY2, activated carbon as well as their composites are given in Fig. 7. It may be observed that activated carbon had the highest water capacity at temperatures below about 160 °C, while it had the lowest capacity above 200 °C. The presence of activated carbon in the composites had a positive impact on the water capacities of the composites, which mostly exceeded those of the original zeolite, to some extent. The NaY2-AC1 composite with the lower amount of activated carbon exhibited higher water capacity than the original zeolite and NaY2-AC2 composite at most of the measurement temperatures. This behavior could be related to the presence of some hydroxysodalite zeolite (as observed by XRD) in the NaY2-AC2 composite prepared by using the higher amount of activated carbon. Another explanation could be that the amount of activated carbon in the composite did not increase in proportion with the amount of activated carbon initially added to the zeolite synthesis mixture. No significant change was observed in the water capacities when two consecutive TG measurements were performed, indicating the stability of all the samples.

The water capacities at 100 °C and 350 °C may be seen more clearly from Table 2. It may be observed that activated carbon had quite higher hydrophobicity and water capacity at 100 °C when compared to the zeolite and composites. On the other hand, at 350 °C, the NaY2-AC1 composite had the highest water capacity. The water capacity of this composite was higher than that of the original zeolite by about 9% and 14% at the relatively high and low temperatures, respectively. Smaller improvements of 4% and 5% were observed for the NaY2-AC2 composite at the lower and higher temperatures, respectively. The hydrophobicity increased slightly by 4% for the NaY2-AC1 composite

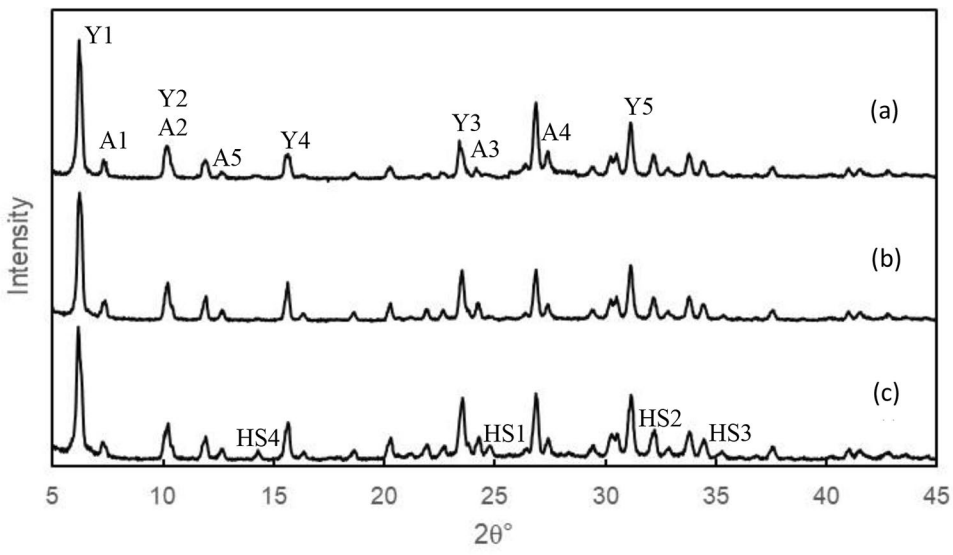

Fig. 5 XRD patterns of (a) zeolite NaY2, (b) NaY2-AC1 composite and (c) NaY2-AC2 composite. Y, A and HS denote zeolites Y, A and hydroxysodalite, respectively

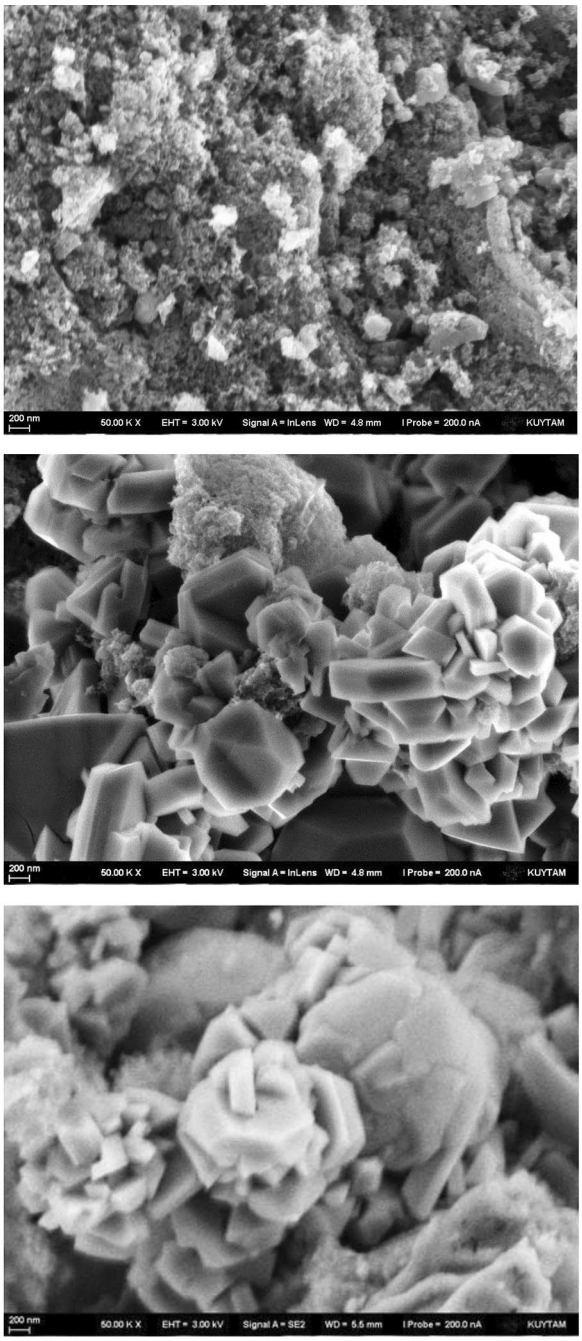

Fig. 6 FEGSEM pictures of (a) activated carbon, (b) NaY2-AC1 composite and (c) NaY2-AC2 composite

while there was no significant change for the NaY2-AC2 composite. When the logarithmic curve in Fig. 1 is taken into consideration, zeolite-activated carbon composites still remained below the curve, though some improvement was obtained.

Calculations were also made by using the water capacities of the original NaY2 zeolite, activated carbon and their weight percentages to determine the water capacity of the composite NaY2-AC1. The amount of activated carbon in the composite was taken as 10 wt%, as determined by EDX analysis. Accordingly, the calculated water capacity at 100 °C was determined to be almost equal to that obtained experimentally for the composite NaY2-AC1. On the other hand, the calculated water capacity at 350 °C was determined as 0.197 g/g adsorbent, which was about 13% lower than the value obtained experimentally. This result indicates that the interface between the zeolite and activated carbon in the composite obtained by zeolite crystallization may affect the sorption performance of the composite. At the interface, the chemical bonding between the zeolite and activated carbon can lead to the formation of a structure different than those of the pure materials. Such an interface, representing a third phase, may have different water sorption properties than the zeolite and activated carbon, leading to these results obtained. The observation of interfacial effects was previously made between zeolite and polymers, forming mixed matrix membranes. For such membranes, the experimental permeabilities were determined to be much different than the values predicted by theoretical models and the results could not be represented by using only the two pure phases [65]. Since an extra zeolite phase existed in the composite NaY2-AC2, a similar calculation was not made for this sample. In any case, the water capacity of NaY2-AC2 composite at 350 °C was higher than that of the original zeolite, too, indicating the possible effect of the interface. It should be remembered that both hydroxysodalite and activated carbon have quite lower water capacities than zeolite NaY2 at 350 °C.

5 Conclusions

A logarithmic curve in a plot of hydrophobicity vs. water capacity was proposed to describe the competency of adsorption performances of various adsorbents for different applications, such as adsorption heat pumps. Aluminosilicate zeolites generally remained well below this logarithmic curve, indicating the necessity of some improvement in their hydrophobicity. These materials may be very useful for a variety of applications, including those involving water adsorption. Although some zeolites have notable water adsorption capacity, their regeneration temperatures are generally too high. In this study, composites were shown theoretically and experimentally to be able to improve the adsorption performances of zeolites. For a composite to be of practical use, it should combine the stability and fast adsorption kinetics of zeolites with the relatively low regeneration temperatures and relatively high water capacities of other adsorbents.

It was observed that the water capacities of the NaY zeolite-salt composites obtained by salt impregnation were

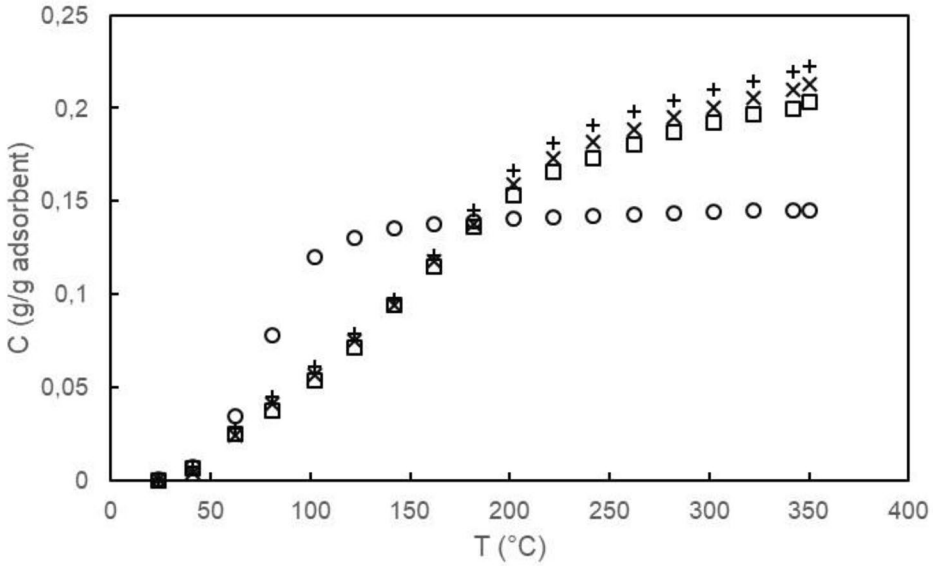

Fig. 7 TG curves of (▢) zeolite NaY2, (o) activated carbon, (+) NaY2-AC1 composite and (x) NaY2-AC2 composite

notably higher than those of the original zeolite at both relatively low and high temperatures. Zeolite-salt composites may eliminate the stability problem of salts, favoring the use of these materials in water sorption applications. Improvements were also obtained for the water capacities of NaY zeolite-activated carbon composites obtained after zeolite crystallization. An interface between the zeolite and activated carbon, with water sorption properties different than the pure materials, may be responsible for the unexpected increase observed in the water capacities of the composites at relatively high temperatures. It is important to note that, due to the existence of an interface, the water capacity of a composite prepared by chemical treatment may be superior to that of a 'so called' composite, simply obtained by the physical mixing of the same components. Composites of different materials and other preparation methods/conditions may also be tested for further possible improvements.

Supplementary Information The online version contains supplementary material available at https://doi.org/10.1007/s10450-024-00459-6.

Author contributions MT: Conceptualization, methodology, validation, writing- original draft preparation, CAO: Conceptualization, investigation, writing- reviewing and editing.

Funding Open access funding provided by the Scientific and Technological Research Council of Türkiye (TÜBİTAK). This work was supported by ITU Scientific Research Projects Unit (Grant # 45079). Open access funding provided by the Scientific and Technological Research Council of Türkiye (TÜBİTAK).

Data availability No datasets were generated or analysed during the current study.

Declarations

Conflict of interest The authors declare no conflict of interest.

Ethical approval Not applicable.

References

1. Zheng, X., Ge, T.S., Wang, R.Z.: Recent progress on desiccant materials for solid desiccant cooling systems. Energy. **74**, 280–294 (2014)
2. Stach, H., Mugele, J., Janchen, J., Weiler, E.: Influence of cycle temperatures on the thermochemical heat storage densities in the systems water/microporous and water/mesoporous adsorbents. Adsorption. **11**, 393–404 (2005)
3. Glaznev, I., Ponomarenko, I., Kirik, S., Aristov, Y.: Composites $CaCl_2$/SBA-15 for adsorptive transformation of low temperature heat: Pore size effect. Int. J. Refrig. **34**, 1244–1250 (2011)
4. Huang, H., Oike, T., Watanabe, F., Osaka, Y., Kobayashi, N., Hasatani, M.: Development research on composite adsorbents applied in adsorption heat pump. Appl. Therm. Eng. **30**, 1193–1198 (2010)
5. Zhao, H.Z., Lei, M., Liu, T., Huang, T.H., Zhang, M.: Synthesis of composite material HKUST-1/LiCl with high water uptake for water extraction from atmospheric air. Inorg. Chim. Acta. **511**, 119842 (2020)

6. Sapienza, A., Glaznev, I.S., Santamaria, S., Freni, A., Aristov, Y.I.: Adsorption chilling driven by low temperature heat: New adsorbent and cycle optimization. Appl. Therm. Eng. **32**, 141–146 (2012)
7. Yan, T.S., Li, T.X., Xu, J.X., Wang, R.Z.: Water sorption properties, diffusion and kinetics of zeolite NaX modified by ion-exchange and salt impregnation. Int. J. Heat. Mass. Tran. **139**, 990–999 (2019)
8. Zhao, H.Z., Liu, T., Wang, Z.Y., Li, Q.W., Wu, T.H., Zhang, M.: Preparation and characterization of composite adsorbent LiCl/zeolite 13X for adsorption system. Int. J. Environ. Sci. Te. **18**, 2693–2702 (2021)
9. Kim, S.K., Cho, K., Rhee, Y.W., Kim, J.N.: Improvement of water adsorption capacity of silico-aluminophosphates by changing Si/Al ratio and impregnation of hygroscopic salt for application of adsorption chiller. B Kor Chem. Soc. **38**, 1427–1434 (2017)
10. Li, H., Zheng, F., Wang, J., Zhou, J., Huang, X., Chen, L., Hu, P., Gao, J.-M., Zhen, Q., Bashir, S., Liu, J.L.: Facile preparation of zeolite-activated carbon composite from coal gangue with enhanced adsorption performance. Chem. Eng. J. **390**, 124513 (2020)
11. Fernández-Reyes, B., Morales-Jiménez, S., Muñoz-Senmache, J.C., Vega-Santander, D.R., Hernández-Maldonado, A.J.: Single- and multi-component adsorption of selected contaminants of emerging concern from water and some of their metabolites onto hierarchical porous copper(II)-zeolite -activated carbon composite. Micropor Mesopor Mater. **312**, 110355 (2021)
12. Candamano, S., Policicchio, A., Conte, G., Abarca, R., Algieri, C., Chakraborty, S., Curcio, S., Calabrò, V., Crea, F., Agostino, R.G.: Preparation of foamed and unfoamed geopolymer/NaX zeolite/activated carbon composites for CO_2 adsorption. J. Clean. Prod. **330**, 129843 (2022)
13. Erdogan, F.O.: Carbon dioxide and methane adsorption behaviour of zeolite/biomass-based activated carbon and zeolite/multi-walled carbon nanotube composites. Int. J. Environ. Anal. Chem. **102**, 7523–7541 (2022)
14. Shojaei, M., Esmaeili, H.: Ultrasonic-assisted synthesis of zeolite/activated carbon@MnO2 composite as a novel adsorbent for treatment of wastewater containing methylene blue and brilliant blue. Environm Monit. Assess. **194**, 279 (2022)
15. Radman, H.M., Dabbawala, A.A., Ismail, I., Alwahedi, Y.F., Polychronopoulou, K., Vaithilingam, B.V., Singaravel, G.P., Morin, S., Berthod, M., Alhassan, S.M.: Influence of salt on nanozeolite-Y particles size synthesized under organic template-free condition. Micropor Mesopor Mater. **282**, 73–81 (2019)
16. Sun, Y.Y., Spiess, A., Jansen, C., Nuhnen, A., Gokpinar, S., Wiedey, R., Ernst, S.J., Janiak, C.: Tunable LiCl@UiO-66 composites for water sorption-based heat transformation applications. J. Mater. Chem. A. **8**, 13364–133745 (2020)
17. Han, B., Chakraborty, A.: Highly efficient adsorption desalination employing protonated-amino-functionalized MOFs. Desalination. **541**, 116045 (2022)
18. Mlonka-Mędrala, A., Hasan, T., Kalawa, W., Sowa, M., Sztekler, K., Pinto, M.L., Mika, L.: Possibilities of using zeolites synthesized from fly ash in adsorption chillers. Energies. **15**, 7444 (2022)
19. Wu, H., Yao, Y., Liu, D.: A modified Guggenheim-Anderson-Boer model for analyzing water sorption in coal. Chem. Eng. J. **451**, 138760 (2023)
20. Yang, F., Shi, R., Huang, H., Zhang, Z., Guo, X., Qiao, Z., Zhong, C.: Nanochannel engineering in metal–organic frameworks by grafting sulfonic groups for boosting proton conductivity. Appl. Energy Mater. **5**, 3235–3241 (2022)
21. Fu, G., Wu, P., Yang, J., Zhang, S., Huai, X.: Cr-doped UiO-66 with enhanced water adsorption for adsorption heat transformation. Micropor Mesopor Mater. **331**, 111642 (2022)
22. Volavšek, J., Pliekhov, O., Pliekhova, O., Mali, G., Logar, N.Z.: Study of water adsorption on EDTA-modified LTA zeolites. Nanomaterials. **12**, 1352 (2022)
23. Gu, X., Han, G., Yang, Q., Liu, D.: Confinement–unconfinement transformation of ILs in IL@MOF composite with multiple adsorption sites for efficient water capture and release. Adv. Mater. Interfaces. **9**, 354 (2022). 2102G
24. Sztekler, K., Mlonka-Mędrala, A., Khdary, N.H., Kalawa, W., Nowak, W., Mika, L.: Possibility of advanced modified-silica-based porous materials utilisation in water adsorption processes—A comparative study. Energies. **15**, 368 (2022)
25. dos Santos, B.F., Cecilia, J.A., Bastos-Neto, M., Rodríguez-Castellón, E., de Azevedo, D.C.S., Vilarrasa-García, E.: Insights into optimized synthesis conditions of hollow microspheres of silica for water vapor adsorption. Chem. Eng. Res. Des. **177**, 583–593 (2022)
26. Wang, L., Wang, K., An, H.-T., Huang, H., Xie, L.-H., Li, J.-R.: A hydrolytically stable Cu(II)-based metal–organic framework with easily accessible ligands for water harvesting. Appl. Mater. Interfaces. **13**, 49509–49518 (2021)
27. Chen, R., Liu, J.: Competitive coadsorption of ammonia with water and sulfur dioxide on metal-organic frameworks at low pressure. Build. Environ. **207**, 108421 (2022)
28. Yang, T.Y., Ge, L.R., Ge, T.S., Zhan, G.W., Wang, R.Z.: Binder-free growth of aluminum-based metal-organic frameworks on aluminum substrate for enhanced water adsorption capacity. Adv. Funct. Mater. **32**, 2105267 (2022)
29. Chairunnisa, Miksik, F., Miyazaki, T., Thu, K., Miyawaki, J., Nakabayashi, K., Wijayanta, A.T., Rahmawati, F.: Development of biomass based-activated carbon for adsorption dehumidification. Energy Rep. **7**, 5871–5884 (2021)
30. Dabbawala, A.A., Reddy, K.S.K., Mittal, H., Al Wahedi, Y., Vaithilingam, B.V., Karanikolos, G.N., Singaravel, G., Morin, S., Berthod, M., Alhassan, S.M.: Water vapor adsorption on metal-exchanged hierarchical porous zeolite-Y. Micropor Mesopor Mater. **326**, 111380 (2021)
31. Tahraoui, Z., Nouali, H., Marichal, C., Forler, P., Klein, J., Daou, T.J.: Zeolite-Polymer composite materials as water scavenger. Molecules. **26**, 4815 (2021)
32. Li, Y., Wang, H.T., Zhao, Y.L., Lv, J., Zhang, X., Chen, Q., Li, J.R.: Regulation of hydrophobicity and water adsorption of MIL-101(cr) through post-synthetic modification. Inorg. Chem. Commun. **130**, 108741 (2021)
33. Hunter, K.M., Kelly, M., Wagner, J.C., Kalaj, M., Cohen, S.M., Xiong, W., Paesani, F.: Simulation meets experiment: Unraveling the properties of water in metal-organic frameworks through vibrational spectroscopy. J. Phys. Chem. **125**, 12451–12460 (2021)
34. Lou, L.T., Xu, M., Huai, X.L., Huang, C.F., Liu, Z.L.: Composite MWCNT/MIL-101 (cr)/$CaCl_2$ as high-capacity water adsorbent for long-term thermal energy storage. Front. Mater. **8**, 653933 (2021)
35. Chairunnisa, Miksik, F., Miyazaki, T., Thu, K., Miyawaki, J., Nakabayashi, K., Wijayanta, A.T., Rahmawati, F.: Enhancing water adsorption capacity of acorn nutshell based activated carbon for adsorption thermal energy storage application. Energy Rep. **6**, 255–263 (2020)
36. Kim, S.H., Cho, K., Kim, J.N., Beum, H.T., Yoon, H.C., Lee, C.H.: Improvement of cooling performance of water adsorption chiller by using aluminophophate adsorbent. Micropor Mesopor Mat. **309**, 110572 (2020)
37. Xu, M., Liu, Z.L., Huai, X.L., Lou, L.T., Guo, J.F.: Screening of metal-organic frameworks for water adsorption heat transformation using structure-property relationships. RSC Adv. **10**, 34621–34631 (2020)

38. Panda, D., Kumar, E.A., Singh, S.K.: Introducing mesoporosity in zeolite 4A bodies for rapid CO_2 capture. J. CO2 Util. **40**, 101223 (2020)
39. Feng, L., Ye, F., Ning, X.Y., Zhou, M., Hou, H.B.: Water adsorption and magnetic properties of Mn-II-MOFs assembled by triazine-based polycarboxylate and 4, 4 '-bipy. J. Solid State Chem. **284**, 121204 (2020)
40. Elsayed, E., Anderson, P., Al-Dadah, R., Mahmoud, S., Elsayed, A.: MIL-101(cr)/calcium chloride composites for enhanced adsorption cooling and water desalination. J. Solid State Chem. **277**, 123–132 (2019)
41. Ristic, A., Kranj, A., Logar, N.Z.: New water adsorbent for adsorption driven chillers. Proc. ISES Eurosun Conf., Int. Solar Energy Soc., Rapperswil, pp. 704–709. (2018)
42. Lenzen, D., Zhao, J.J., Ernst, S.J., Wahiduzzaman, M., Inge, A.K., Frohlich, D., Xu, H.Y., Bart, H.J., Janiak, C., Henninger, S., Maurin, G., Zou, X.D., Stock, N.: A metal-organic framework for efficient water-based ultra-low-temperature-driven cooling. Nat. Commun. **10**, 3025 (2019)
43. Wang, C., Luo, Y.H., He, X.T., Hong, D.L., Wang, J.Y., Chen, F.H., Chen, C., Sun, B.W.: Porous high-valence metal-organic framework featuring open coordination sites for effective water adsorption. Inorg. Chem. **58**, 3058–3064 (2019)
44. Entezari, A., Ge, T.S., Wang, R.Z.: Water adsorption on the coated aluminum sheets by composite materials (LiCl plus LiBr)/silica gel. Energy. **160**, 64–71 (2018)
45. Dabbawala, A.A., Tzitzios, V., Sunny, K., Polychronopoulou, K., Basina, G., Ismail, I., Pillai, V., Tharalekshmy, A., Stephen, S., Alhassan, S.M.: Synthesis of nanoporous zeolite-Y and zeolite-Y/GO nanocomposite using polyelectrolyte functionalized graphene oxide. Surf. Coat. Technol. **350**, 369–375 (2018)
46. Gao, M.Z., Wang, J., Rong, Z.H., Shi, Q., Dong, J.X.: A combined experimental-computational investigation on water adsorption in various ZIFs with the SOD and RHO topologies. RSC Adv. **8**, 39627–39634 (2018)
47. Basina, G., Aishamia, D., Polychronopoulou, K., Tzitzios, V., Balasubramanian, V., Dawaymeh, F., Karanikolos, G.N., Wahedi, A.: Hierarchical AlPO4-5 and SAPO-5 microporous molecular sieves with mesoporous connectivity for water sorption applications. Surf. Coat. Technol. **353**, 378–386 (2018)
48. Askalany, A.A., Ernst, S.J., Hugenell, P.P.C., Bart, H.J., Henninger, S.K., Alsaman, A.S.: High potential of employing bentonite in adsorption cooling systems driven by low grade heat source temperatures. Energy. **141**, 782–791 (2017)
49. Truong, B.N., Park, J., Kwon, O.K., Park, J.: Water adsorption capacity enhancement of ferroaluminophosphate (FAPO(4)-5) by impregnation of $CaCl_2$. Mater. Lett. **215**, 137–139 (2018)
50. Liu, R.L., Gong, T., Zhang, K., Lee, C.: Graphene oxide papers with high water adsorption capacity for air dehumidification. Sci. Rep. **7**, 9761 (2017)
51. Nan, Y., Lin, R.H., Liu, J.X., Crowl, T.B., Ladshaw, A., Yiacoumi, S., Tsouris, C., Taylarides, L.L.: Adsorption equilibrium and modeling of water vapor on reduced and unreduced silver-exchanged mordenite. Ind. Eng. Chem. Res. **56**, 8095–8102 (2017)
52. Chen, H.Y., Ding, J., Wang, W.L., Wei, X.L., Lu, J.L.: Water adsorption characteristics of MCM-41 post-modified by Al grafting and cations doping: Equilibrium and kinetics study. Adsorption. **23**, 113–120 (2017)
53. Alonso-Buenaposada, I.D., Calvo, E.G., Montes-Moran, M.A., Narciso, J., Menendez, J.A., Arenillas, A.: Desiccant capability of organic xerogels: Surface chemistry vs porous texture. Micropor Mesopor Mater. **232**, 70–76 (2016)
54. Sharma, P., Song, J.S., Han, M.H., Cho, C.H.: GIS-NaP1 zeolite microspheres as potential water adsorption material: Influence of initial silica concentration on adsorptive and physical/topological properties. Sci. Rep. **6**, 22734 (2016)
55. Zheng, X., Wang, R.Z., Ge, T.S., Hu, L.M.: Performance study of SAPO-34 and FAPO-34 desiccants for desiccant coated heat exchanger systems. Energy. **93**, 88–94 (2015)
56. Kamegawa, T., Mizuno, A., Yamashita, H.: Hydrophobic modification of SO3H-functionalized mesoporous silica and investigations on the enhanced catalytic performance. Catal. Today. **243**, 153–157 (2015)
57. Frohlich, D., Henninger, S.K., Janiak, C.: Multicycle water vapour stability of microporous breathing MOF aluminium isophthalate CAU-10-H. Dalton Trans. **4**, 15300–15304 (2014)
58. Canivet, J., Bonnefoy, J., Daniel, C., Legrand, A., Coasne, B., Farrusseng, D.: Structure-property relationships of water adsorption in metal-organic frameworks. New. J. Chem. **38**, 3102–3111 (2014)
59. Alcaniz-Monge, J., Perez-Cadenas, M., Lozano-Castello, D.: Influence of pore size distribution on water adsorption on silica gels. J. Porous Mater. **17**, 409–416 (2010)
60. Bedia, J., Rodriguez-Mirasol, J., Cordero, T.: Water vapour adsorption on lignin-based activated carbons. J. Chem. Technol. Biotechnol. **82**, 548–557 (2007)
61. Wang, C., Guo, H.D., Leng, S.Z., Yu, J.L., Feng, K., Cao, L.Y., Huang, J.F.: Regulation of hydrophilicity/hydrophobicity of aluminosilicate zeolites: A review. Crit. Rev. Solid State Mater. Sci. **46**, 330–348 (2021)
62. Whiting, G.T., Grondin, D., Stosic, D., Bennici, S., Auroux, A.: Zeolite–$MgCl_2$ composites as potential long-term heat storage materials: Influence of zeolite properties on heats of water sorption. Sol Energy Mater. Sol Cells. **128**, 289–295 (2014)
63. Tatlier, M., Atalay-Oral, C., Bayrak, A., Maraş, T., Erdem, A.: Impact of ion exchange on zeolite hydrophilicity/hydrophobicity monitored by water capacity using thermal analysis. Thermochim Acta. **713**, 179240 (2022)
64. Treacy, M.M.J., Higgins, J.B.: Collection of Simulated XRD Powder Patterns for Zeolites. Elsevier, Amsterdam (2001)
65. Tatlier, M., Atalay-Oral, C.: Estimation of interphase properties of various mixed matrix membranes. Comp. Interf. **26**, 825–837 (2019)